

Instituto Tecnológico y de Estudios Superiores de Occidente

Repositorio Institucional del ITESO

rei.iteso.mx

Departamento del Hábitat y Desarrollo Urbano

DHDU - Artículos y ponencias con arbitraje

2015-09

Seismic vulnerability and failure modes simulation of ancient masonry towers by validated virtual finite element models

Preciado, Adolfo

Preciado, A. (2015). "Seismic vulnerability and failure modes simulation of ancient masonry towers by validated virtual finite element models". *Journal of Engineering Failure Analysis*, 57: pp. 72-87

Enlace directo al documento: <http://hdl.handle.net/11117/3471>

Este documento obtenido del Repositorio Institucional del Instituto Tecnológico y de Estudios Superiores de Occidente se pone a disposición general bajo los términos y condiciones de la siguiente licencia:
<http://quijote.biblio.iteso.mx/licencias/CC-BY-NC-ND-2.5-MX.pdf>

(El documento empieza en la siguiente página)

1 **“Seismic Vulnerability and Failure Modes Simulation of Ancient Masonry Towers**
2 **by Validated Virtual Finite Element Models”**

3 Adolfo Preciado

4 Professor and Researcher at the Polytechnical University of Guadalajara, Mexico (UPZMG)
5 preciadoqa@yahoo.es
6

7 **ABSTRACT**

8 Seismic protection of ancient masonry towers is a topic of great concern among the scientific
9 community. A methodology for the seismic vulnerability assessment of all types of towers and
10 slender unreinforced masonry structures (e.g. light houses and minarets) is presented. The
11 approach is developed by four validated 3D FEM models representative of European towers. The
12 models are subjected to linear elastic investigations to establish load carrying capacity and
13 dynamic properties for validation against similar towers. Seismic simulations are developed
14 through intensive nonlinear static pushover analyses. From the assessments, the failure modes
15 and overall seismic response of the towers are obtained. Low tensile strength of masonry and
16 large openings at belfries have significant influence on the seismic behavior, resulting in a quasi-
17 brittle failure. All the towers presented an imminent high vulnerability to seismic actions. The
18 few investigations reported in literature on the seismic behavior of towers are focused on in-plane
19 behavior, disregarding out-of-plane behavior and toe crushing, both aspects are investigated in
20 this paper. The more flexible towers are close to present toe crushing in both planes. The failure
21 mechanisms are validated with reported post-earthquake observations on real damaged towers.

22 ***Keywords:*** *Strong earthquakes; historical towers; old masonry; failure mechanisms; damage*
23 *assessment; seismic vulnerability; validated virtual models; nonlinear Finite Element Method*

24 **1. CULTURAL HERITAGE IN EARTHQUAKE PRONE COUNTRIES**

25 Most of cultural heritage (masonry monuments) of the world is located in earthquake (EQ) prone
26 zones with different levels of seismic hazard and source characteristics (e.g. Mexico, Chili, Italy,
27 Portugal, Turkey, China and New Zealand). These monuments were built following empirical
28 rules to mainly withstand the vertical loading induced by their self weight, disregarding the effect
29 of horizontal inertia forces induced by EQs. This was due to the limitations in materials
30 technology and knowledge about EQs and structural behavior in that time. The construction of
31 historical buildings was carried out by empirical rules transmitted from generation to generation
32 mainly by means of geometrical approaches and by trial and error about structural stability. The
33 lack of knowledge, quasi-brittle and heavy materials such as masonry and other factors make
34 historical buildings extremely vulnerable to suffer partial or total collapse even by EQs of low
35 intensity. This trend has been observed through centuries and nowadays (Fig. 1) almost after
36 every EQ of considerable intensity (e.g. 2003 M7.5 in Colima, Mexico; 2009 M6.3 in L'Aquila,
37 Italy and 2011 M6.3 in Christchurch, New Zealand). There is a high interest among the nations
38 and scientific community in preserving the cultural heritage of humanity.

39 EQ assessment of cultural heritage located in seismic areas is an issue of very intensive research
40 in recent years. The main difficulties on the seismic analysis of these buildings arise from the
41 complex geometry, high heterogeneity, anisotropy and heavy mass of masonry. Moreover, the
42 poor behavior of masonry due to its low tensile strength if compared to the compressive one,
43 induces cracking since very low lateral loads. All these factors in combination with the EQ
44 loading tends to separate the structure into macro-blocks that behave independently with different
45 failure mechanisms. Degradation of masonry through time (long-term heavy loads) is another

46 important factor affecting the seismic behavior of old buildings, reducing the strength of masonry
47 and the possible structural failure even in static conditions.

48 **2. SEISMIC VULNERABILITY ASSESSMENT OF CULTURAL HERITAGE**

49 The seismic vulnerability assessment of a historical building is a complex task if compared to
50 another existing building as explained in the works of Preciado (2011), Barbieri et al. (2013),
51 Foraboschi (2013), Preciado et al. (2014) and Preciado and Orduña (2014). This section is aimed
52 at describing the most important and current methodologies reported in literature for assessing in
53 a satisfactory way the seismic vulnerability of a historical masonry building. It is explained the
54 need of using a masonry material model able to represent its nonlinear behavior, and the use of
55 linear elastic analyses just as model verification and validation. Moreover, the analytical
56 approaches are compared against Finite Element Method (FEM), highlighting advantages and
57 drawbacks.

58 **2.1 Historical masonry**

59 Masonry is known as the combination of units (natural and carved stones, bricks, adobe and
60 combinations) with a mixture named mortar that aims to bind the construction units together and
61 to fill the gaps between them. Mortars in ancient structures are mainly integrated of clay or lime
62 in combination with water. In some cases other materials or compounds used to be added to the
63 mortar (e.g. ashes, fibers, blood and cactus extract) for increasing its capacity of adherence,
64 resistance, durability and malleability during the construction. This additives aimed at reducing
65 the contraction of adobe units and mortar generated by drying, and to enhance its resistance to
66 climate change effects. Unreinforced masonry (URM) is one of the most durable and ancient
67 materials commonly found worldwide in historical constructions. This is due to the fact that the
68 use of this especial material as structure goes back to the first civilizations that populated the

69 earth. From the ancient time until now, masonry has been widely appreciated around the world by
70 different important factors such as availability, durability, bioclimatic characteristics, and its low
71 cost if compared to other materials (e.g. steel or reinforced concrete). In the construction of
72 historical structures multiple typologies of masonry were used depending on many factors such
73 as availability of materials, structural element (arch, wall, buttress, dome, or vault), construction
74 technique and appearance.

75 **2.2 Seismic vulnerability assessment methods**

76 Inside the framework of the seismic risk management there are two main stages recommended to
77 be follow as a measure to achieve the protection of cultural heritage. These stages correspond to
78 the seismic risk assessment and its reduction. Nowadays there is an enormous variety of
79 methodologies to assess the seismic risk (or seismic vulnerability) of buildings ranging from
80 simple (e.g. empirical or qualitative) to more complex quantitative approaches (e.g. analytical-
81 experimental). The selection of the most suitable method depends on factors such as number of
82 buildings, importance, available data, and aim of the study. The empirical methods satisfactorily
83 allow the evaluation of a single building or a complete city in a fast and qualitative way before or
84 after the occurrence of a seismic event (EQ scenarios). For assessing the vulnerability of an
85 historical building the procedure is different and more in detail than in the qualitative and rough
86 evaluations by empirical methods. It is more complex, requires more computer resources and
87 especial equipment, and represents more time consuming. The literature recommends applying a
88 hybrid approach by combining empirical, analytical and experimental methods to obtain more
89 reliable and quantitative results about the amount of damage caused by the EQ over the structure.

90 Seismic vulnerability assessment of buildings is an issue of most importance at present time and
91 is a concept widely used in works related to the protection of buildings. Nevertheless, there is not

92 a rigorous and widely accepted definition of it. In general terms, vulnerability measures the
93 amount of damage caused by an EQ of given intensity over a structure. However, “amount of
94 damage” and “seismic intensity” are concepts without a clear and rigorous numerical definition
95 (Orduña et al., 2008). There is no general approach for assessing the seismic vulnerability of a
96 complex historical building. One approximation may consists of obtaining at a first instance all
97 the relevant information such as identification of structural elements, damages, plans, historical
98 analysis and restorations, as well as experimental vibration tests. Furthermore, with the obtained
99 information is possible to construct a 3D geometrical model with computational tools. After
100 building the initial 3D model (e.g. FEM, Limit Analysis, etc.), the mechanical properties of
101 materials constituting the structure and boundary conditions (BCs) are assigned. Together with a
102 suitable constitutive material model able to satisfactory represent the nonlinear behavior of URM,
103 the model is statically or dynamically assessed. These evaluations are linear or nonlinear
104 depending on the aim of the study and the action under analysis (e.g. self weight, seismic loading,
105 wind, etc.) to define the levels of damage at the structure (vulnerability). Once the seismic
106 assessment of the building is developed and identified its behavior, failure modes and key
107 vulnerable parts, the most suitable retrofitting measure is proposed to improve the overall seismic
108 capacity.

109 **2.3 Linear vs nonlinear approaches**

110 In the case of assessing the seismic vulnerability of masonry buildings, linear analyses suffer
111 from the absence of correlation between linear behavior and ultimate limit state. More
112 specifically, the stress results of a linear analysis are not significant, since a masonry structure
113 does not fail due to excessive stresses but due to a mechanism (either rotating or translating)
114 (Blasi and Foraboschi, 1994). Nonlinear static analyses by means of the pushover approach relate

115 the resistance and energy-dissipation capacity to be assigned to the structure to the extent to
116 which its non-linear response is to be exploited. Therefore, non-linear static analyses account for
117 both the actual force-resisting system of the building, in particular the overstrength, and the
118 actual energy-dissipation system of the building, in particular not only the plastic dissipation
119 (Foraboschi and Vanin, 2013). In brief, linear elastic analyses are only used to verify the load
120 carrying capacity of a certain structure in terms of distribution of stresses, as well as to compare
121 the numerical frequencies with the experimental ones for model calibration/updating.

122 **2.4 Analytical approaches vs Finite Element Method**

123 In the framework of the FEM analysis, three main modeling strategies for masonry are identified
124 to be the most used in the relevant literature. The micro-modeling of single elements (unit, mortar
125 and interface) and meso-modeling (unit and interface), are suitable for the analysis of small
126 structures, e.g. Lofti and Shing (1994) and Lourenço and Rots (1997). The large amount of time
127 for the generation of the detailed structural model and high calculation effort prevent their use in
128 the seismic analysis of sophisticated and large-scale structures as in the case of historical
129 constructions. On the other hand, the macro-modeling (smeared, continuum or homogenized),
130 considers masonry as an anisotropic composite material, e.g. Gambarotta and Lagomarsino
131 (1997), Lourenço et al. (1998) and Schlegel (2004). This simplifies the generation of the
132 structural model, and due to the significantly reduction of the degrees of freedom, less calculation
133 effort is needed, being considered as suitable for the seismic analysis of large historical
134 constructions. Macro-modeling of masonry through analytical models is also gaining the
135 attention of the scientific community for static nonlinear analysis purposes. Among them are the
136 3D limit analysis approach by rigid macro-blocks (Orduña and Lourenço, 2005a and b) (Orduña
137 et al. 2008) and the strut-and-tie model (Foraboschi and Vanin, 2013). The first approach is based

138 on a rigid-perfectly plastic material that does not need parameters of stiffness and softening, only
139 strength parameters. On the other hand, it is not possible to evaluate the displacements and
140 deformations of the structure, which are fundamental for seismic energy dissipation assessments.

141 The strut-and-tie modeling approach was developed for reinforced concrete members and can
142 include externally reinforced concrete members (Biolzi et al., 2013). The strut-and-tie modeling
143 approach is supported by the lower bound theorem of the limit analysis, as well as by the
144 maximum stiffness or minimum deformation energy criteria (Blasi and Foraboschi, 1994).
145 Actually, the original form of the lower bound theorem refers to an elasto–plastic constitutive law
146 of the material, which does not include masonry. However, the lower bound theorem can be
147 extended to masonry structures, under the assumption that masonry has an elasto-plastic
148 compression behavior (or perfectly elastic) and a no-tension behavior, which is an assumption
149 that suits masonry adequately (Foraboschi and Vanin, 2013). However, FEM modeling is still the
150 most powerful tool and recommended to assess the vulnerability of large historical constructions
151 against EQs. This is due to its capability to calibrate the model with real experimental data and
152 possibility to simulate a nonlinear dynamic analysis, taking into account the EQ characteristics,
153 damping and dissipation of energy.

154 **3. SEISMIC VULNERABILITY OF OLD MASONRY TOWERS**

155 Existing ancient masonry towers (AMT) with different characteristics and functions are
156 distributed all over the world and constitute a relevant part of the architectural and cultural
157 heritage of humanity. These vertical structures were built either isolated or commonly included in
158 different manners into the urban context, such as built as part of churches, castles, municipal
159 buildings and city walls. Bell and clock towers (see Fig. 2), also named civic towers, were built
160 quite tall for informing people visually and with sounds about time and extraordinary events such

161 as civil defence or fire alarm, and to call the community to social meetings. Another reason that
162 led to the construction of tall civic towers in the medieval cities of Italy was that they were seen
163 as a symbol of richness and power of the great families. Strong damage or complete loss suffered
164 by the cultural patrimony due to EQs has been occurring through the history of humanity.

165 **3.1 Fundamental aspects determining the seismic vulnerability of towers**

166 The occurrence of unexpected and unavoidable events such as EQs has demonstrated that AMT
167 are one of the most vulnerable structural types to suffer strong damage or collapse as depicted in
168 Figure 1. Their protection is a topic of great concern among the scientific community. This
169 concern mainly arises from the observed damages after every considerable EQ and the need and
170 interest to preserve this cultural heritage. Although the recent progress in technology, seismology
171 and EQ engineering, the preservation of these quasi-brittle and massive monuments stills
172 represents a major challenge. Masonry towers in all their uses (bell, clock and medieval towers)
173 are highly vulnerable to suffer strong damage or collapse in EQ conditions, even when subjected
174 to seismic events of low to moderate intensity.

175 These vertical structures are slender by nature, the slenderness (H/L) of towers is the single most
176 decisive factor affecting their seismic performance, characterized by a ductile behavior where
177 bending and low tensile strength of masonry determinate the overall performance. The position of
178 a tower in the urban context is an important aspect that influences the vulnerability of the
179 structure (Sepe et al., 2008). These boundary conditions could strongly modify its seismic
180 behavior and have big impact in the generation of different failure modes. Non-isolated towers
181 were commonly built as part of churches or next to another building. Adjacent walls or façades
182 with different height than the tower and the lack of connection between elements by the poor
183 tensile strength of masonry could generate during an EQ a detachment of the different bodies. In

184 addition, the seismic vulnerability of towers is increased by certain important aspects such as soil
185 conditions, large openings at belfries, nonlinear behavior of masonry, lack of good connection
186 between structural elements, high vertical loading and progressive damage. These fundamental
187 aspects determine the seismic vulnerability of towers in terms of behavior and failure
188 mechanisms that differentiate them from most of compact historical constructions.

189 AMT were built as most of the historical buildings to mainly withstand the vertical loading
190 generated by their self-weight. The thickness of walls used to be determined by following
191 empirical rules transmitted from generation to generation by trial and error mainly based on the
192 height and observed EQ damage. These empirical rules led to the construction of walls with
193 enormous thicknesses higher than 2 m. The roof system of towers was usually made of the same
194 material of the walls, even when reduced thicknesses were considered, the elevated mass of
195 masonry generated problems of instability that could lead to collapse even during the
196 construction works. For avoiding heavy roofs, it is quite frequent to especially find in Italy
197 masonry towers with a plane roof system integrated by wooden beams and fired-clay bricks.
198 AMT are slender structures under high vertical loading due to the height, wall thickness, presence
199 of a tall roof system, high density of masonry and large bells. This loads lead to a concentration
200 of high compressive stresses mainly at the base. All these issues and moreover taking into
201 account the deterioration of masonry through the centuries make AMT extremely vulnerable to
202 suffer a sudden collapse by exceeding the intrinsic compressive strength. These sudden collapses
203 have been occurring since centuries ago in this type of structures. The most famous cases are
204 reported in Binda et al. (1992), Macchi (1993), GES (1993) and Binda (2008). They relate to the
205 collapses of the bell tower of “Piazza San Marco”, Venice in, the civic tower of Pavia in 1989
206 and the bell tower of the church of “St. Maria Magdalena” in Goch, Germany in 1992.

207 **3.2 Post-earthquake observations and typical failure modes of towers**

208 The identification of seismic behavior and failure mechanisms of AMT subjected to in-plane and
209 out-of-plane loading is a complicated task. This identification strongly depends on many factors
210 such as soil and boundary conditions, geometrical characteristics and mechanical properties of
211 masonry (mortar and units), level of vertical loading and the EQ characteristics. All these factors
212 play an important role in the determination of the seismic behavior and failure mechanisms of
213 AMT. Compared to other compact structures, masonry towers mainly fail ductile in a
214 predominant bending behavior due to the excessive slenderness ($\text{height} / \text{length} > 4$). Due to this,
215 and the heavy mass, the lateral vibration at the top of the tower during an EQ is considerably
216 more amplified than the base, inducing important displacements and inertia forces. This behavior
217 could cause different failure mechanisms as illustrated in Figure 1. Meli (1998) describes that
218 during an EQ, masonry towers present important horizontal top displacements. Bending
219 generates horizontal cracks but rarely the overturning of the structure. This is due to the
220 alternation of the movement that causes an opening and closing effect of these cracks, dissipating
221 with the impact an important part of the EQ energy.

222 On the other hand, in bell towers, the presence of large openings at belfry could increase the
223 vulnerability of the structure, being more frequent the failure by shear. Due to the strong damage,
224 the belfry could collapse by instability, endangering the adjacent buildings and mainly people
225 who could be inside or in the surroundings. The last almost happened due to the M7.5 Colima EQ
226 in 2003, where one belfry collapsed by overturning on the basketball court of a neighbor building
227 (see Fig. 1b). The remaining damaged belfry was removed during the rehabilitation and
228 retrofitting works, and in the end it was decided to leave the church without belfries for security
229 reasons (Preciado, 2011).

230 Alcocer et al. (1999) describe that the key behavior of bell towers during EQs is dominated by in-
231 plane failure in the direction of the façade. The out-of-plane failure of towers is generally less
232 important and is only regarded with the detachment of the façade from the nave. Curti et al.
233 (2008) observed in 31 Italian bell towers damaged by the 1976 Friuli EQs that the belfry is the
234 most vulnerable part of the tower due to the presence of large openings, natural bending behavior
235 and low tensile strength of masonry. This amplifies the seismic motion causing critical effects at
236 the top part of the tower. Peña and Meza (2010) developed post-earthquake observations in 172
237 Colonial churches with bell towers after two major EQs occurred in 1999 in Puebla and Oaxaca,
238 Mexico. The authors identified that the main damage in masonry towers is at belfry, due to the
239 great openings and heavy mass of these structures, with no masonry crushing at the base of the
240 tower. Based on observed damage on AMT after considerable EQs occurred in Italy,
241 Lagomarsino et al. (2002) propose the damage mechanisms of Figure 3. The body damage of
242 Figure 3a corresponds to horizontal cracking out-of-plane due to bending behavior and diagonal
243 cracking by shear stresses in-plane, leading to overturning over the nave. The type of damage of
244 Figure 3b consists of vertical cracking in both planes due to horizontal tension, resulting in the
245 detachment of walls and collapse by instability. On the other hand, the damage mode of Figure 3c
246 is represented by alternated diagonal cracking in-plane due to shear which could be repaired. The
247 damages at belfries are mainly characterized by horizontal and diagonal cracking due to the
248 presence of large openings, leading to the collapse by overturning (Figs. 3d-f). In brief, the author
249 of this paper may conclude that the main failure mechanisms presented in bell towers due to EQ
250 loading are the following: (1) horizontal cracking at the tower's body due to bending behavior,
251 (2) stepped or diagonal cracking at the tower's body by shear stresses, (3) vertical cracking at the
252 tower's body due to horizontal tensile stresses induced by the detachment from other vertical

253 elements (e.g. the façade or nave of a church) (4) partial or total collapse of belfries due to shear
254 stresses and bending behavior, and (5) masonry crushing at the compressed toes.

255 **4. SEISMIC FAILURE AND BEHAVIOR SIMULATION OF OLD MASONRY TOWERS**

256 The main objective of this paper is to develop a methodology for the seismic vulnerability
257 assessment of all types of towers and slender URM structures (e.g. light houses and minarets),
258 through the correct simulation of failure modes and behavior. The simulation of seismic response
259 and failure modes is developed through validated FEM models of four virtual historical masonry
260 towers commonly found in Europe with variations in geometry, roof system and boundary
261 conditions (see Fig. 4). As a first approximation, the generated 3D FEM models of the towers are
262 evaluated by linear elastic procedures to obtain in relatively simple way information about the
263 load carrying capacity and dynamic characteristics (natural frequencies and vibration modes). In
264 order to obtain representative models of real AMT, the numerical results are validated with
265 theoretical back ground and experimental results on similar towers reported in literature. Before
266 starting with the static and dynamic nonlinear analyses of the towers, the capability of the applied
267 masonry model to simulate the nonlinear behavior of masonry is validated with selected
268 experimental examples reported in literature. Since the towers are theoretical, the seismic hazard
269 is determined at a first instance in qualitative terms by the damage grades of the European
270 Macroseismic Scale (EMS-98) proposed by Grünthal (1998) and the limit states of the
271 performance-based design (PBD) philosophy for different EQ intensities. The seismic action is
272 evaluated in quantitative terms by the seismic coefficient obtained in the analyses. As a final
273 approximation, intensive numerical simulations through a series of nonlinear static analyses are
274 carried out for the EQ evaluation of the AMT. The results are validated with reported key-
275 behavioral characteristics and observed EQ damage.

276 **4.1 Characteristics of the virtual AMT and FEM models**

277 The general view and dimensions of the virtual AMT under study are illustrated in Figure 4. The
278 towers were selected taking into account common AMT (see Fig. 2) with variations in roof
279 system, height, boundary conditions and openings at belfry. The main objective is to obtain
280 different failure mechanisms and behavior, in order to compare them with the observed damage
281 after moderate to strong EQs. The first two towers (AMT 1-2) of Figure 5, correspond to bell
282 towers with large openings at the four sides of belfry and tall and heavy masonry roof. The tower
283 AMT 1 (Fig. 4a) is isolated and the AMT 2 (Fig. 4b) has neighbor buildings (non-isolated). The
284 last two towers (AMT 3-4) of Figure 4 are isolated and have light timber roof. The AMT 3 model
285 is representative of bell towers with only one opening at belfry (Fig. 4c) and AMT 4 of medieval
286 towers (Fig. 4d) with no belfry (see Table 1). Table 1 presents the 3D FEM models of the
287 proposed virtual AMT, which are developed by means of the commercial software ANSYS®. The
288 first two models (AMT 1-2) have the same geometry and roof system but different BCs. The
289 interaction between neighbor buildings at the AMT 2 model is taken into account at the East
290 façade (at 10 m height) and at the North one (at 15 m height). The simulated interaction with
291 neighbor buildings is illustrated in Figure 4b and Table 1b. The third and fourth models (AMT 3-
292 4) have a light timber roof common of this type of structures that could be neglected in the
293 analyses (see Figs. 4c-d and Table 1c-d).

294 The selected element for walls and roofs is Shell43, which has four nodes and four thicknesses
295 with six degrees of freedom (DOF) at each node. This element can represent in-plane and out-of-
296 plane behavior and has plasticity and creep capabilities. In the generation of the four numerical
297 models the following main assumptions were taken into account: (1) because the type of
298 foundation and soil properties are not considered, all the base nodes were assumed as fixed. (2)

299 The main mechanical properties of the AMT were proposed by taking into account average
300 values reported in literature. The selected masonry was considered as carved stone with lime
301 mortar, with an average density of 2000 kg/m³ and a Young's modulus of 2000 MPa. The
302 Poisson's ratio was held constant and equal to 0.15. The compressive strength was assumed to be
303 3.5 MPa and the tensile strength 0.25 MPa. (3) At the non-isolated model AMT 2 (Table 1b), the
304 interaction with neighbor buildings in the North and East façades was simulated by a uniform
305 distribution of linear elastic springs of constant stiffness (275 Combin14 elements). To simulate
306 the interaction induced by neighbor masonry buildings it is proposed Ec. 1, based on the works of
307 Pandey and Meguro (2004), Crisafulli and Carr (2007) and Mondal and Jain (2008), where the
308 authors assess the lateral stiffness contribution on masonry infill panels. The axial spring stiffness
309 K_{sp} is assumed to be equal to a fraction γ of the total stiffness of a masonry block.

$$310 \quad K_{sp} = \gamma \frac{E_m A_m}{T_m} \quad (1)$$

311 Where E_m is the elastic modulus of masonry, A_m is the area of a composite masonry block of 1x1
312 m (4 springs) and T_m is the wall thickness. The factor γ is recommended in literature to be
313 estimated between 0.50 and 0.75 depending on the researcher when calibrating the model. During
314 the calibration process it is decided to use a factor of 0.30, resulting in a spring stiffness of 100
315 kN/mm. This value is in good agreement with the proposed by Ivorra and Pallares (2006), where
316 the authors experimentally evaluated the lateral stiffness contribution of masonry façades in old
317 bell-towers.

318 **4.2 Validation of the virtual AMT by linear static and dynamic analyses**

319 Static and dynamic linear evaluations such as vertical loading and modal were firstly developed
320 to obtain an important progress on the seismic vulnerability assessment without the convergence

321 problems related to nonlinear analyses. These linear elastic approximations permit to determine
322 the presence and magnitude of tensile and compressive stresses at the masonry structure by
323 vertical loading, as well as the frequencies and vibration modes in the modal analysis. In the
324 generation of structural models of complex historical constructions there are many assumptions
325 and uncertainties regarding the determination of geometry, material properties, and boundary
326 conditions. In this case, the linear analyses could be used to calibrate (or up-date) the initial
327 model with the experimental data by adjusting geometry, material properties and interaction with
328 adjacent buildings. This permits to obtain models more representative of the structure under
329 study, and with this, a reliable seismic vulnerability assessment. In case of masonry towers the
330 vertical load represents an important factor in the seismic behavior, because these structures were
331 constructed by empirical rules only to withstand their self-weight. In historical towers, usually
332 the zone most over stressed is the bottom part. High compressive stresses could generate local
333 failure of masonry and may be the trigger of sudden collapse as explained in Section 3.1. The
334 models with triangular roof (AMT 1-2) present the same vertical distribution of stresses because
335 they have the same mass (interaction with neighbor buildings has no influence), therefore only
336 one tower is presented (Fig. 5a). In case of the other two towers (AMT 3-4) with timber roof
337 (Figs. 5b and c), there is a small variation of mass by the presence of openings. However, the
338 maximum values are present at the doors due to the reduction of the resistant area. The two
339 towers with triangular roof present tensile stresses at the base of the cover (Fig. 5a). This trend is
340 in agreement with real behavior observed in similar masonry towers. The roof bends due to the
341 heavy weight and height, generating vertical cracking similar to domes. Therefore is more
342 common to observe in this type of towers tall triangular roofs made of timber. The vertical
343 analyses have revealed that the towers (AMT 1-4) are in linear conditions, because the levels of
344 compressive stresses are lower than the intrinsic strength and tensile stresses are not present in

345 large zones. These results allowed the validation of the FEM models regarding static conditions,
346 concluding that the towers are stable to satisfactorily resist their own self weight as most of
347 historical constructions.

348 The linear investigations were extended to dynamic analyses in order to obtain a first estimation
349 of the dynamic response of the four virtual towers. As in the case of the vertical loading analyses,
350 the modal evaluations of FEM models are relatively fast due to the progress of recent decades on
351 computational tools. As a first stage, the dynamic parameters of the isolated and non-isolated
352 towers with masonry roof are numerically obtained. The resulting vibration modes of both towers
353 are similar, therefore only the modes of the isolated tower (AMT 1) are depicted in Figure 6a.
354 The natural frequencies of the non-isolated model (AMT 2) are higher (lower periods) as
355 expected, due to the increment of stiffness (about 24 % in the N-S direction and 8 % in the E-W)
356 generated by the assumed contact with neighbor buildings (Table 2). Analyzing the results of
357 Figure 6a and Table 2, it could be observed that the two fundamental vibration modes of both
358 towers correspond to a general bending. This low frequencies (high periods of about 1 s) and
359 vibration modes, are representative of real behavior of slender and tall structures as AMT, which
360 are highly vulnerable to EQ motions. The higher modes represent torsion and a particular
361 problem of vertical vibration due to the tall and heavy roof. Afterwards, the natural frequencies
362 and vibration modes of the isolated towers with timber roof (AMT 3-4) are numerically obtained
363 as presented in Figure 6b and Table 2. In this case the vibration modes and frequencies are
364 similar as in the case of the towers with heavy roof.

365 To validate the numerical natural frequencies of the virtual towers obtained in the modal
366 analyses, an extensive literature review was developed. Bachmann et al. (1997) and Casolo
367 (1998) describe in their works that the natural frequencies of slender masonry towers are

368 measured between 0.9 and 2 Hz (periods between 0.5 and 1.11 s). The Spanish Standard NCSE
 369 (2002) considers a masonry structure as slender when its first natural period is comprised
 370 between $0.75 \text{ s} < T < 1.25 \text{ s}$ ($0.8 \text{ Hz} < f < 1.33 \text{ Hz}$). The same Standard proposes an analytical
 371 formula to approximately assess the first frequency ω of masonry bell towers (see Eq. 2). Where
 372 L corresponds to the plan dimension in the vibration direction and H is the height of the tower.
 373 The suitability and efficiency of this equation as a first and quick estimation (or validation of
 374 numerical and experimental results) of the first natural frequency of real masonry bell towers
 375 have been proved by many researchers, e.g. Ivorra and Pallares (2006), Ivorra et al. (2008),
 376 Bayraktar et al. (2009), Preciado (2011).

$$377 \quad \omega_1 = \frac{\sqrt{L}}{0.06 H \sqrt{\frac{H}{2L + H}}} \quad (\text{Hz}) \quad (2)$$

378 As a result of applying Ec. 2 on the four FEM models of the virtual towers in the vibration
 379 direction E-W, the isolated tower with masonry roof (AMT 1) is supposed to have a first natural
 380 frequency of 1.119 Hz. The result is in good agreement with the obtained in the numerical
 381 simulation for the same direction (1.051 Hz). For the case of the non-isolated tower with masonry
 382 roof (AMT 2) is expected a greater first natural frequency as a consequence of the contact with
 383 neighbor buildings. The increment in stiffness induced by neighbor buildings is obtained in the
 384 numerical simulations (see Table 2). For the case of the two towers with timber roof (AMT 3-4),
 385 the equation does not consider the influence of openings in the total mass. Therefore both first
 386 natural frequencies in the E-W direction are the same and correspond to 1.334 Hz (modal
 387 analysis: 1.064 Hz and 1.083 Hz respectively). As a final validation, the obtained natural
 388 frequencies by modal analyses and Eq. 2 are compared to experimental results in similar masonry
 389 towers reported in literature (see Table 3). It is worth noting that the frequency reduces with the

390 increment in height, being the structure more slender, and as a consequence more flexible. The
391 masonry tower of 35 m assessed by Slavik (2002) has a first natural frequency of 1.10 Hz, which
392 is in very good agreement to the presented by the AMT 3-4 models of 32 m (1.076 and 1.064 Hz
393 respectively). The same trend is observed between the first frequencies of the 45.5 m isolated
394 tower (1.05 Hz) evaluated by Abruzzese et al. (2009) and AMT 1-2 of 45 m (1.046 Hz).

395 **4.3 Seismic failure mechanisms of the AMT by nonlinear static analyses**

396 In the nonlinear analyses through FEM models, the homogenized masonry material model
397 developed by Gambarotta and Lagomarsino (1997) is implemented. This model is capable to
398 simulate the main failure mechanisms and behavior of masonry structures in static and dynamic
399 conditions, and is integrated in ANSYS[®] by subroutines. The model is based on the macro-
400 modeling approach, which is considered as appropriate for the seismic assessment of large
401 historical constructions. The suitability of the material model in masonry structures has been
402 proved through numerical simulations by Calderini and Lagomarsino (2006), Urban (2007),
403 Sperbeck (2009) and Preciado (2011) against experimental results reported in literature, e.g. Van
404 der Pluijm and Vermeltoort (1991), Raijmakers and Vermeltoort (1992) and Vermeltoort and
405 Raijmakers (1993). The model is based on a micromechanical approach where masonry is
406 assumed as a composite medium made up of an assembly of units connected by bed mortar
407 joints. The contribution of head joints is not considered. The constitutive equations are obtained
408 by homogenizing the composite medium and on the hypothesis of plane stress condition. The
409 model is characterized by three yield surfaces: tensile failure, sliding of mortar joints and
410 compressive failure of units. In brief, if tensile stresses act in mortar bed joints $\sigma_y \geq 0$, three
411 damage modes may become active: failure of units, sliding and failure of mortar bed joints. On
412 the other hand, if mortar joints are under compressive stresses $\sigma_y < 0$, then both damage

413 mechanisms of units and mortar are activated. The needed masonry material parameters are
414 described in Table 4. In order to assess the seismic response of an historical building is
415 recommended to obtain the material parameters through detailed experimental campaigns. This is
416 always a complex and expensive task, mainly due to the heterogeneity of masonry, lack of
417 representative samples and the need of non-destructive tests. In case that it is not possible to
418 obtain all the material parameters, the ones proposed and calibrated through numerical
419 simulations by Preciado (2011) are recommended.

420 The towers of Figure 2 are subjected to the pushover method with the integrated material model.
421 The FEM models are firstly loaded with the gravitational force, and in a subsequent stage, the
422 horizontal force is applied under monotonically increased top displacement control. From the
423 analysis it is possible to obtain the complete capacity curve and failure mechanisms during the
424 analysis, especially to capture the nonlinear (plastic) range. In the analyses the displacement-
425 based load pattern is applied through a considerable number of steps and sub-steps especially in
426 the nonlinear range in order to attain convergence. The time of computational calculation for
427 every analysis is in the order of 8 hours by means of a standard desktop work station. In order to
428 have comparative indicators of performance, it is included at the capacity curves the EQ
429 performance limit states established by the European Code (EC-8) (Eurocode 8, 2004); the
430 damage limit state (DLS) at first yielding; significant damage limit state (SDLS) representing
431 significant damage and the ultimate limit state (ULS) near collapse. Moreover, these limit states
432 at the capacity curves are correlated to the damage grades (DG) DG 2, DG 3 and DG 4 proposed
433 by the European Macroseismic Scale (EMS-98) reported in Grünthal (1998). For having
434 quantitative indicators of performance at the capacity curves, it is included the seismic coefficient
435 (SC) determined by the ratio between the ultimate lateral force and the vertical loading. The SC is

436 typically expressed as a fraction or percentage of the gravity (g). The main drawback of this
437 indicator is that only the lateral strength of the structure is evaluated, disregarding the
438 displacement and ductility which is extremely important in the EQ assessment of structures for
439 energy dissipation capabilities.

440 In both towers with masonry roof AMT 1 and AMT 2 (Figs. 7 and 8), the analyses illustrate a
441 failure mode governed by diagonal cracking due to in-plane shear stresses at the large openings
442 (front and back) at belfries. This is due to the reduction of the resistant area at this weakened part.
443 The final failure mode in both towers is suddenly formed by the extension of the in-plane
444 diagonal cracks at openings of belfries (Figs. 7b and 8b). These large cracks lead to the collapse
445 of belfries, placing in a situation of danger the adjacent buildings and people inside or in the
446 surroundings. Masonry crushing at the in-plane and out-of-plane compressed toes is not
447 observed, due to the fact that these towers present quasi-brittle behavior by belfry failure. The
448 maximum compressive stresses of about 1.4 MPa, being lower than the intrinsic strength (3.5
449 MPa). Figure 9 illustrates the capacity curves of the two towers with triangular roof (AMT 1 and
450 AMT 2), including the damage grades of the EMS-98 and the limit states of EC-8. It is worth
451 noting that the linear behavior of both towers is different. The non-isolated tower (AMT 2) is
452 stiffer than the isolated one (AMT 1) due to the interaction with adjacent buildings as it was
453 observed in the modal analysis, reaching the yielding (DG 2) at a displacement of 40 mm and a
454 lateral force of 2220 kN. By the other hand, the isolated tower approximately presents 22 % more
455 lateral force and about 33 % more displacement capacity ($F= 2700$ kN and $U= 53$ mm) at the
456 same yielding stage. In the nonlinear range, both towers present similar lateral load capacity but
457 different displacement. This behavior continues until both towers reach ultimate conditions,
458 showing the isolated one about 10 % more displacement ($F= 4350$ kN and $U= 115$ mm).

459 The failure mechanisms of the virtual masonry towers with timber roof AMT 3 and AMT 4 are
460 illustrated in Figures 10 and 11. The medieval tower AMT 4 presents a global bending behavior
461 represented by the initial formation of horizontal cracks (see Fig. 11a) due to vertical tensile
462 stresses at the base level at a displacement of 155 mm, which corresponds to a DG 3 and a limit
463 state of significant damage (SDLS). The tower reaches an ULS and a damage grade 4 at a
464 displacement of 265 mm. The final collapse mechanism (Fig. 11b) is formed due to the extension
465 of the horizontal cracks. The failure by masonry crushing is not observed, due to the maximum
466 value of stress in the compressed in-plane and out-of-plane toes is in the order of 3.086 MPa,
467 which is lower than the intrinsic strength (3.5 MPa). On the other hand, the isolated bell tower
468 with timber roof and openings (AMT 3) presents a different behavior as illustrated in Figure 10.
469 The tower shows at a displacement of 185 mm the initial formation of horizontal cracks due to
470 vertical tensile stresses as in the case of the medieval tower (AMT 4) but at a different height in
471 both planes of the posterior part (Fig. 10a). The presence of diagonal cracks is evident by shear
472 stresses in the plane of the main door. The tower reaches an ULS at a displacement of 325 mm,
473 represented by a final failure mode due to the extension of horizontal and diagonal cracks (Fig.
474 10b). This tower is close of failing by masonry crushing at the compressed toes in both planes,
475 with a maximum compressive stress of 3.305 MPa. The obtained seismic failure mechanisms
476 through validated virtual models of AMT are characteristic of this type of structures and are in
477 complete agreement with the described in post-earthquake observations (Section 3.2).

478 **4.4 Capacity curves and behavior of the AMT by nonlinear static analyses**

479 The capacity curves of the bell and medieval towers (AMT 3-4) with timber roof including the
480 damage grades (EMS-98) and limit states (EC-8) are illustrated in Figure 12. It could be observed
481 that both towers present similar linear behavior, reaching the yielding (DG 2, DLS) at the same

482 load of 1100 kN and a displacement of 55 mm. The towers present different nonlinear behavior at
483 a DG 3 and SDLS, being more evident the difference in the ultimate limit state (DG 4, ULS). The
484 tower with openings shows about 9% more lateral force and 23% more displacement (F= 1750
485 kN and U= 325 mm) than the tower with no openings. This trend is similar to the numerically
486 results on ancient masonry structures with different configuration reported in Preciado (2011) and
487 the experimental tests of Rajmakers and Vermeltoort (1992) and Vermeltoort and Rajmakers
488 (1993). Comparing the capacity curves of the four FEM models of the virtual towers illustrated in
489 Figures 9 and 12, it is worth noting that the towers with masonry roof are more resistant to lateral
490 loading, but in contrast present less ductile behavior. Table 5 summarizes the results of the
491 seismic evaluation of the four virtual historical masonry towers by the pushover method. The SCs
492 are calculated at ultimate lateral conditions and are presented in Table 6.

493 In the seismic analysis summary of Table 5, it could be observed that in the DLS and DG 2, the
494 four towers present similar displacement, being stiffer the tower with the assumed adjacent
495 buildings. The difference is evident in the lateral carrying capacity, withstanding the stiffer tower
496 (AMT 2) about 100 % more lateral load, and the isolated with masonry roof (AMT 1) about 145
497 %. In the SDLS and DG 3 the towers with masonry roof (AMT 1-2) present more lateral strength
498 capacity but in contrast less ductility. The towers with timber roof (AMT 3-4) show different
499 seismic behavior between them at ultimate conditions (ULS and DG 4), presenting the tower with
500 openings (AMT 3) about 9 % more force and 23 % more displacement.

501 In the summary of SCs of Table 6, it could be observed that the two towers with timber roof
502 (AMT 3-4) have similar vertical loading, with a small variation in the tower with openings AMT
503 3 (less mass). This tower shows more lateral force capacity of about 150 kN due to the different
504 seismic behavior induced by the main door opening. The towers with masonry roof (AMT 1-2)

505 present the same vertical loading because they have the same mass. Regarding lateral force, both
506 towers show similar capacity, with 50 kN more the isolated one (AMT 1). Compared to the
507 towers with masonry roof, the ones with timber show about 2.5 times less force and vertical
508 loading. Because of this relationship, the four towers have similar SC. The obtained low values of
509 SC represent in quantitative terms, the high vulnerability of this type of structures to seismic
510 actions. These SCs are in complete agreement with the typical values of ancient masonry
511 buildings, in the range between 0.1 and 0.3 as mentioned by Meli (1998). In contrast, for
512 seismically designed masonry buildings, the SC is in the range between 0.5 and 0.86. In
513 conclusion, the four virtual historical masonry towers would reach an ULS or collapse under an
514 EQ ground motion of 0.1 g. The SC allows obtaining more reliable results (quantitative) than the
515 qualitative damage indicators. On the other hand, it is not possible to obtain information with this
516 coefficient about maximum displacement capability.

517 **5. CONCLUSIONS**

518 A proposed methodology for the validation of virtual AMT and seismic vulnerability assessment
519 through failure mechanisms and behavior was described. The research was developed through
520 four validated 3D FEM models representative of towers usually found in Europe. As a first
521 approximation on the seismic assessment, the FE models were subjected to linear elastic
522 investigations on their load carrying capacity and dynamic characteristics. These initial analyses
523 permitted to validate the models with theoretical background and experimental data on similar
524 towers reported in literature. This validation plays an important role to obtain models
525 representative of real towers, and with this, more reliable results in the seismic vulnerability
526 evaluation. This validation could be useful when there is no experimental data available to
527 calibrate the model, and when available, as a practical pre-calibration. The described strategy to

528 simulate the interaction with neighbor buildings is envisaged to simplify the model construction
529 and the nonlinear analyses, because normally the modeling of non-isolated towers is done by
530 including the complete façade or nave of the church. Intensive numerical simulations by
531 nonlinear static analyses were carried out. The seismic analyses by the pushover approach
532 successfully permitted to obtain the overall seismic response of the towers, represented by the
533 capacity curves and the in-plane and out-of-plane failure modes. The huge impact of the low
534 tensile strength of masonry and large openings at belfries on the seismic behavior was observed,
535 failing the AMT 1 and AMT 2 models in a quasi-brittle mode by shear stresses. The medieval
536 tower AMT 4 presented the characteristic bending behavior with horizontal cracks in-plane and
537 out-of-plane. The similar tower with openings AMT 3 presented a mixed failure mode of bending
538 and shear stresses at the bottom (attracted by the main door opening), being more resistant and
539 ductile. The same trend was observed in the validation of the material model stage and was
540 corroborated with reported experimental observations.

541 The few investigations reported in literature on the seismic behavior of AMT are mainly focused
542 on the in-plane behavior and disregard horizontal cracking out-of-plane and masonry crushing at
543 the tower's bottom. The more flexible towers (AMT 3-4) were close to present crushing in both
544 planes. The behavior and damage types were validated with the seismic vulnerability aspects
545 described in Section 3.1 and the reported post-earthquake observations on masonry towers of
546 Section 3.2. The capability of the applied model to simulate the nonlinear behavior of masonry
547 and collapse mechanisms at masonry towers in post-earthquake observations showed a very good
548 agreement. The seismic hazard was included in qualitative terms at the capacity curves for
549 different DGs and limit states, and quantitatively by the SC. A drawback of the SC is that
550 ductility is not considered, which is quite important to evaluate energy dissipation. The three

551 approaches permitted to satisfactorily assess the seismic vulnerability of the four AMT. All of
552 them presented an imminent high vulnerability to seismic actions.

553

554 REFERENCES

555 Abruzzese, D., Miccoli, L. and Vari, A. (2009). “Dynamic investigations on medieval masonry
556 towers: Seismic resistance and strengthening techniques.” Proceedings of the 1st Int. Conf. on
557 Protection of Historical Buildings (PROHITECH), Rome, Italy.

558 Alcocer, S. M., Aguilar, G., Flores, L., Bitrán, D., Durán, R., López, O. A., Pacheco, M. A.,
559 Reyes, C., Uribe, C. M. and Mendoza, M. J. (1999). “The Tehuacan EQ of June 15th, 1999 (in
560 Spanish).” National Center for the Prevention of Disasters IEG/03/99, Mexico.

561 Bachmann, H., Ammann, W. and Deischl, F. (1997). “Vibration problems in structures: Practical
562 Guidelines.” Springer Verlag, Berlin, 50-55.

563 Barbieri, G., Biolzi, L., Bocciarelli, M., Fregonese, L. and Frigeri, A. (2013) “Assessing the
564 seismic vulnerability of a historical building.” *Engineering Structures*, 57: 523–535.

565 Bayraktar, A., Türker, T., Sevim, B., Altunisik, A. C. and Yildirim, F. (2009). “Modal parameter
566 identification of Hagia Sophia bell-tower via ambient vibration test.” *Journal of Nondestructive
567 Evaluation* 28: 37-47.

568 Binda, L., Gatti, G., Mangano, G., Poggi, C. and Sacchi-Landriani, G. (1992). “The collapse of
569 the civic tower of Pavia: A survey of the materials and structure.” *Masonry International* 11-20.

570 Binda, L. (2008). “Learning from failure: Long-term behaviour of heavy masonry structures.”
571 Polytechnic of Milano, Italy. Published by WIT press, GB.

572 Biolzi, L., Ghittoni, C., Fedele, R. and Rosati, G. (2013). “Experimental and theoretical issues in
573 FRP-concrete bonding.” *Construction Building Materials*, 41: 182–190.

574 Blasi, C. and Foraboschi, P. (1994). “Analytical approach to collapse mechanisms of circular
575 masonry arch.” *Journal of Structural Engineering (ASCE)*, 120(8): 2288-2309.

576 Calderini, C. and Lagomarsino, S. (2006). "A micromechanical inelastic model for historical
577 masonry." *Journal of Earthquake Engineering* 10(4): 453-479.

578 Casolo, S. (1998). "A three-dimensional model for the vulnerability analysis of a slender
579 medieval masonry tower." *Journal of Earthquake Engineering*, Vol. 2, No. 4: 487-512.

580 Crisafulli, F. J. and Carr, A. J. (2007). "Proposed macro-model for the analysis of infilled frame
581 structures." *Bulletin of the New Zealand Society for Earthquake Engineering*, 40(2): 69-77.

582 Curti, E., Parodi, S. and Podesta, S. (2008). "Simplified models for seismic vulnerability analysis
583 of bell towers." *Proceedings of the 6th International Conference on Structural Analysis of*
584 *Historical Constructions (SAHC)*, July 2-4, 2008, Bath, UK.

585 Eurocode 8 (2004). "Design of structures for earthquake resistance - Part 1: General rules,
586 seismic actions and rules for buildings." European Standard.

587 Foraboschi P. (2013). "Church of San Giuliano di Puglia: Seismic repair and upgrading."
588 *Engineering Failure Analysis* 33: 281-314.

589 Foraboschi, P. and Vanin, A. (2013). "Non-linear static analysis of masonry buildings based on a
590 strut-and-tie modeling." *Soil Dynamics and Earthquake Engineering*, 55: 44-58.

591 Gambarotta, L. and Lagomarsino, S. (1997). "Damage models for the seismic response of brick
592 masonry shear walls." Part I and II. *Earthquake Engineering and Structural Mechanics*, Vol. 26:
593 441-462.

594 Gentile C. and Saisi A. (2007). "Ambient vibration testing of historic masonry towers for
595 structural identification and damage assessment." *Construction and Building Materials* 21: 1311-
596 1321.

597 GES (1993). "Technical opinion about the collapse of the bell tower of St. Maria Magdalena in
598 Goch, Germany ." *Gantert Engineering Studio*.

599 Grünthal, G. (1998). "European Macroseismic Scale EMS-98." *Notes of the European Center of*
600 *Geodynamics and Seismology*, Volume 15, Luxembourg.

601 Ivorra, S. and Pallares F. J. (2006). "Dynamic investigations on a masonry bell tower."
602 *Engineering structures* 28: 660-667.

603 Ivorra, S., Pallares, F. J. and Adam, J. M. (2008). "Experimental and numerical studies on the
604 bell tower of Santa Justa y Rufina (Orihuela-Spain)." Proceedings of the 6th International
605 Conference on Structural Analysis of Historical Constructions (SAHC), Bath, UK.

606 Lagomarsino, S., Podesta, S. and Resemini, S. (2002). "Seismic response of historical churches."
607 12th European Conference on Earthquake Engineering, Paper Reference 123 (Genoa), September
608 9-13, 2002, London, UK.

609 Lofti, H. R. and Shing, P. B. (1994). "Interface model applied to fracture of masonry structures."
610 Journal of Structural Engineering, 120 (1), 63-81.

611 Lourenço, P. B. and Rots, J. (1997). "A multi-surface interface model for the analysis of masonry
612 structures." Journal on Engineering Mechanics, 123 (7), 660-668.

613 Lourenço, P. B., Rots, J. and Blaauwendraad, J. (1998). "Continuum model for masonry:
614 Parameter estimation and validation." Journal on Structural Engineering, 124 (6), 642-652.

615 Lund, J. L., Selby, A. R. and Wilson, J. M. (1995). "The dynamics of bell towers: A survey in
616 northeast England." Proceedings of the 4th International Conference on Structural Repairs and
617 Maintenance of Historical buildings. 2: 45-52.

618 Macchi, G. (1993). "Monitoring medieval structures in Pavia." Structural Engineering
619 International, I/93.

620 Meli, R. (1998). "Structural engineering of the historical buildings (in Spanish)." Civil Engineers
621 Association (ICA) Foundation, A. C., Mexico.

622 Mondal, G. and Jain, S. K. (2008). "Lateral stiffness of masonry infilled reinforced concrete
623 frames with central openings." Earthquake Spectra, 24 (3): 701-723.

624 NCSE (2002). "Spanish Seismoresistant Construction Norm (in Spanish)." General Part and
625 Edification (Spanish standard). Ministry of Foment. Spain.

626 Orduña, A. and Lourenço, P. B. (2005a). "Three-dimensional limit analysis of rigid blocks
627 assemblages. Part I: Torsion failure on frictional interfaces and limit analysis formulation."
628 International Journal of Solids and Structures, 42 (18-19): 5140-5160.

629 Orduña, A. and Lourenço, P. B. (2005b). “Three-dimensional limit analysis of rigid blocks
630 assemblages. Part II: Load-path following solution procedure and validation.” *International*
631 *Journal of Solids and Structures*, 42 (18-19): 5161-5180.

632 Orduña, A., Preciado, A., Galván, J. F. and Araiza, J. C. (2008). “Vulnerability assessment of
633 churches at Colima by 3D limit analysis models.” *Proceedings of the 6th Int. Conference on*
634 *Structural Analysis of Historical Constructions (SAHC)*, Bath, UK.

635 Pandey, B. H. and Meguro, K. (2004). “Simulation of brick masonry wall behavior under in-
636 plane lateral loading using applied element method.” *Proceedings of the 13th Conference on*
637 *Earthquake Engineering*, Paper 1664, Vancouver, Canada.

638 Peña, F. and Meza, M. (2010). “Seismic assessment of bell towers of Mexican colonial
639 churches.” *Proceedings of the 7th International Conference on Structural Analysis of Historic*
640 *Constructions (SAHC)*, October 6-8, 2010, Tongji University, Shanghai, China.

641 Preciado (2011). “Seismic vulnerability reduction of historical masonry towers by external
642 prestressing devices”. Doctoral thesis, Technical University of Braunschweig, Germany and
643 University of Florence, Italy. Published at: <http://www.biblio.tu-bs.de/>

644 Preciado, A., Lester, J., Ingham, J. M., Pender, M. and Wang, G. (2014). “Performance of the
645 Christchurch, New Zealand Cathedral during the M7.1 2010 Canterbury earthquake.”
646 *Proceedings of the 9th International Conference on Structural Analysis of Historical*
647 *Constructions (SAHC)*, Topic 11, Paper 02, Mexico City.

648 Preciado and Orduña (2014). “A correlation between damage and intensity on old masonry
649 churches in Colima, Mexico by the 2003 M7.5 earthquake.” *Journal of Case Studies in Structural*
650 *Engineering*, 2: 1-8.

651 Ramos, L. F., Marques, L., Lourenço, P. B., De Roeck, G., Campos-Costa, A. and Roque, J.
652 (2010). “Monitoring historical masonry structures with operational modal analysis: Two case
653 studies.” *Mechanical Systems and Signal Processing*, 24 (5): 1291-1305.

654 Raijmakers, T. M. J. and Vermeltoort, A. T. (1992). “Deformation controlled tests in masonry
655 shear walls (in Dutch).” Report B-92-1156, TNO-Bouw, Delft, The Netherlands.

656 Schlegel, R. (2004). “Numerical simulations of masonry structures by homogenized and discrete
657 modeling strategies (in German).” Doctoral thesis, University of Weimar, Germany.

658 Russo, G., Bergamo, O., Damiani, L. and Lugato, D. (2010). "Experimental analysis of the Saint
659 Andrea masonry bell tower in Venice: A new method for the determination of tower global
660 young's modulus E." *Engineering Structures*, 32 (2): 353-360.

661 Sepe, V., Speranza, E. and Viskovic, A. (2008). "A method for large-scale vulnerability
662 assessment of historic towers." *Structural control and health monitoring*, 15: 389-415.

663 Slavik, M. (2002). "Assessment of bell towers in Saxony." *Proceedings of the 4th Int.*
664 *Conference on Structural Dynamics (EURODYN)*, September 2-5, Munich, Germany.

665 Sperbeck, S. (2009). "Seismic risk assessment of masonry walls and risk reduction by means of
666 prestressing." *Doctoral thesis*, Technical University of Braunschweig, Germany.

667 Urban, M. (2007). "Earthquake risk assessment of historical structures." *Doctoral thesis*,
668 *Technical University of Braunschweig*, Germany.

669 Van der Pluijm, R. and Vermeltfoort, A. T. (1991). "Deformation controlled tension and
670 compression tests in units, mortar and masonry (in Dutch)." *Report B-91-0561*, The Netherlands.

671 Vermeltfoort, A. T. and Rajmakers, T. M. J. (1993). "Deformation controlled tests in masonry
672 shear walls, Part 2 (in Dutch)." *Report TUE/BKO/93.08*, Eindhoven University of Technology,
673 The Netherlands.

674

675

676

677

678

679

680

681

682 **LIST OF FIGURES**

683 Figure 1: Observed EQ damage on cultural heritage; (a) L'Aquila, Italy in 2009 M6.3; (b)
684 Colima, Mexico in 2003 M7.5 and (c) Christchurch, New Zealand in 2011 M6.3

685 Figure 2: Ancient masonry civic towers; (a) bell-towers and (b) clock tower

686 Figure 3: Observed EQ damage mechanisms at masonry towers; (a-c) at the body of the tower
687 and (d-f) at the level of belfry (Lagomarsino et al., 2002)

688 Figure 4: General view and dimensions (in m) of the four virtual old masonry towers; (a) AMT1
689 heavy roof; (b) AMT 2 heavy roof; (c) AMT 3 light roof and (d) AMT 4 light roof

690 Figure 5: Vertical distribution of stresses at the FEM models (units in MPa); (a) AMT 1-2
691 masonry roof; (b) AMT 3 timber roof and (c) AMT 4 timber roof

692 Figure 6: Top view of vibration modes of the four AMT; (a) AMT 1-2 and (b) AMT 3

693 Figure 7: Isolated tower masonry roof (AMT 1). Principal plastic strain contours (front and back)
694 at a displacement of: (a) 80 mm (DG 3, SDLS) and (b) 115 mm (DG 4, ULS)

695 Figure 8: Non-isolated tower masonry roof (AMT 2). Principal plastic strain contours (front and
696 back) at: (a) 70 mm (DG 3, SDLS) and (b) 105 mm (DG 4, ULS)

697 Figure 9: Isolated and non-isolated bell towers with masonry roof (AMT 1 and AMT 2). Capacity
698 curves with the damage grades of the EMS-98 and limit states EC-8



699

700



(a)



701

702

(b)



(c)

703 Figure 1: Observed EQ damage on cultural heritage; (a) L'Aquila, Italy in 2009 M6.3; (b)

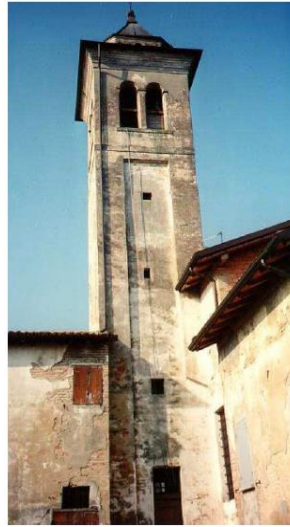
704 Colima, Mexico in 2003 M7.5 and (c) Christchurch, New Zealand in 2011 M6.3

705

706

707

708



709

710

(a)

(b)

711

Figure 2: Ancient masonry civic towers; (a) bell-towers and (b) clock tower

712

713

714

715

716

717

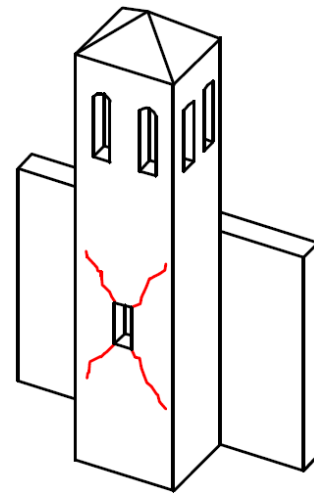
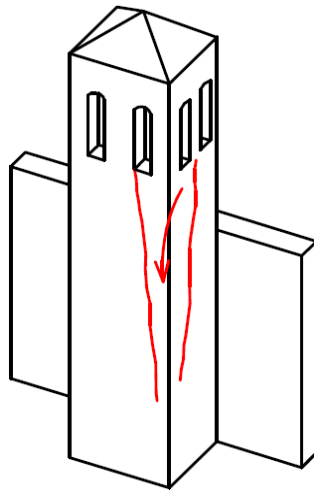
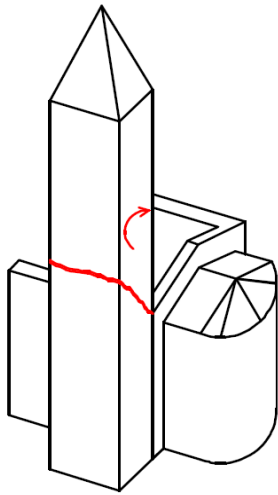
718

719

720

721

722



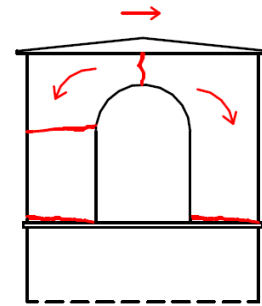
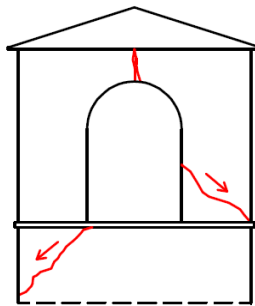
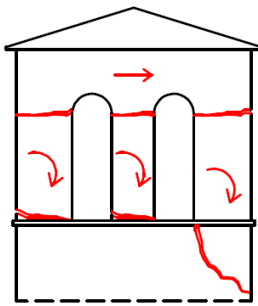
723

724

(a)

(b)

(c)



725

726

(d)

(e)

(f)

727

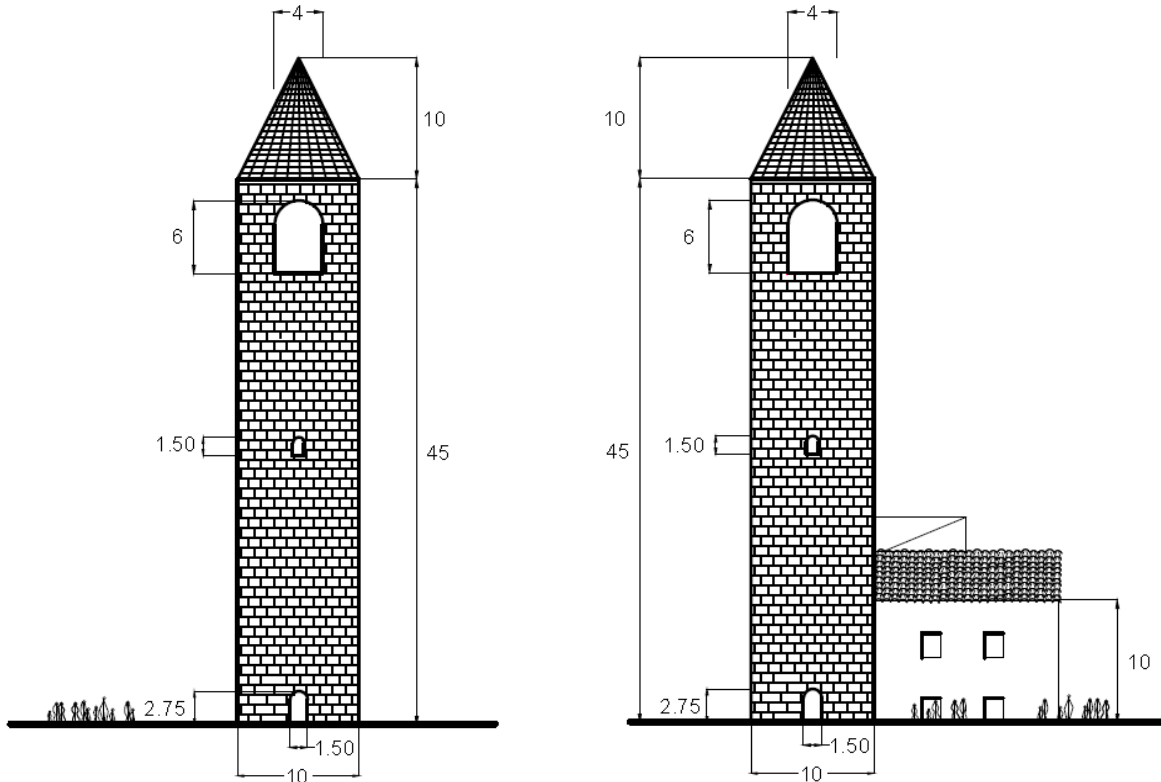
728

729

730

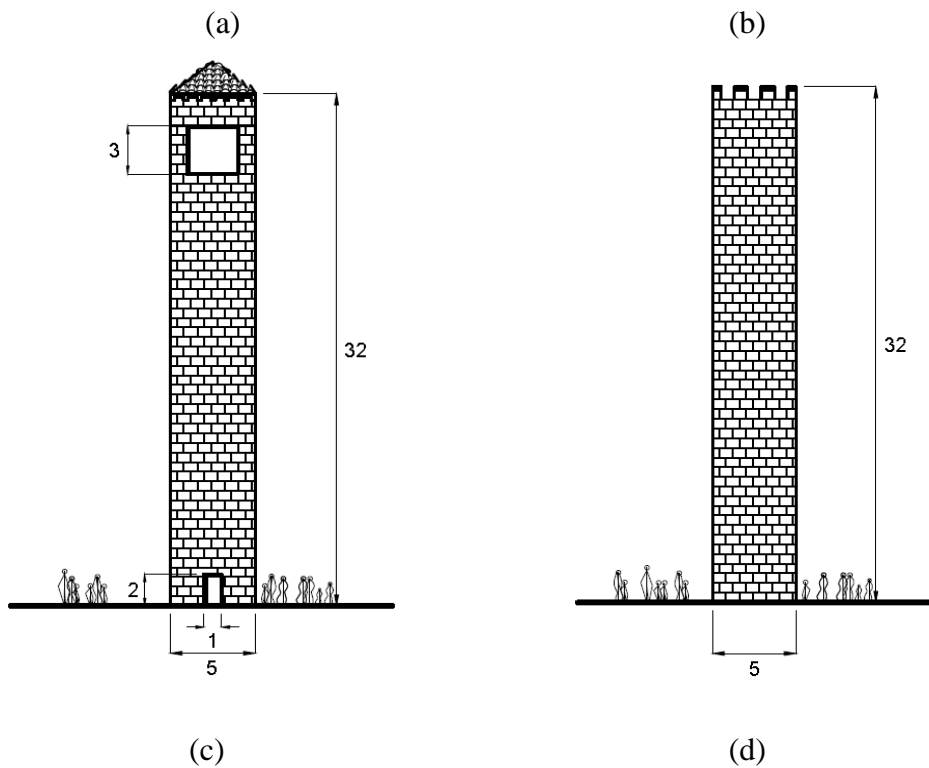
731

Figure 3: Observed EQ damage mechanisms at masonry towers; (a-c) at the body of the tower and (d-f) at the level of belfry (Lagomarsino et al., 2002)



732

733



734

735

736

737

Figure 4: General view and dimensions (in m) of the four virtual old masonry towers; (a) AMT 1 heavy roof; (b) AMT 2 heavy roof; (c) AMT 3 light roof and (d) AMT 4 light roof

738
739
740
741
742
743
744
745
746
747
748
749
750
751

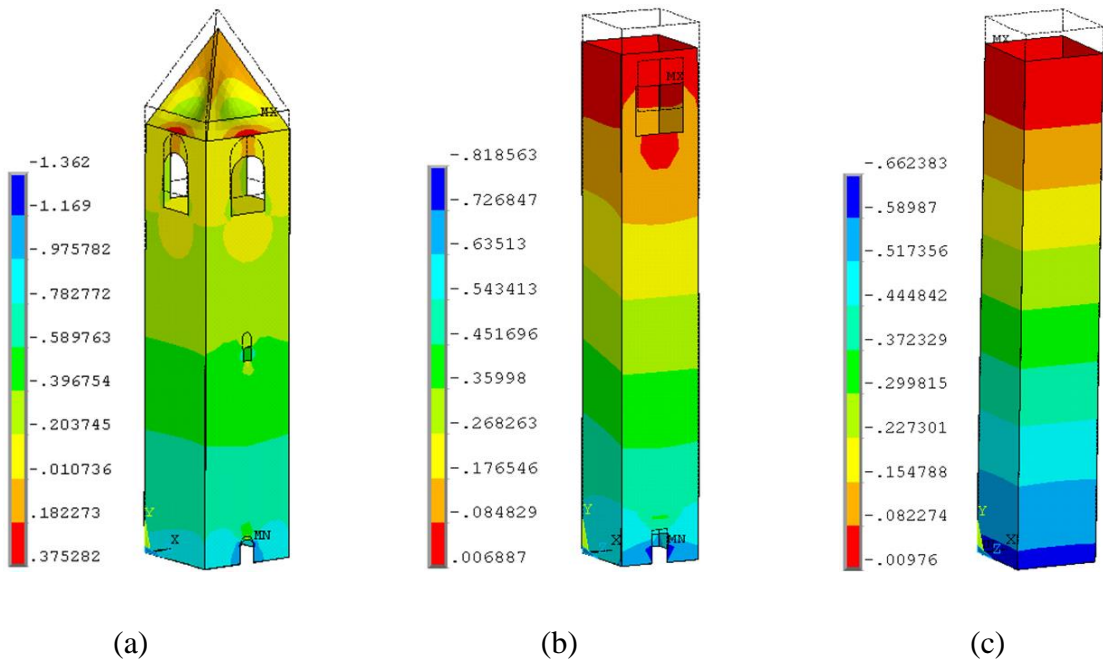


Figure 5: Vertical distribution of stresses at the FEM models (units in MPa); (a) AMT 1-2 masonry roof; (b) AMT 3 timber roof and (c) AMT 4 timber roof



Mode 1

Mode 2

Mode 3

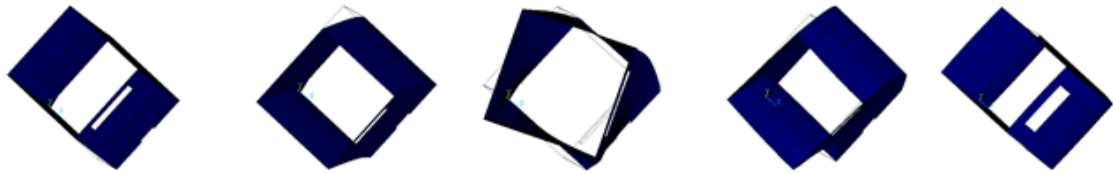
Mode 4

Mode 5

752

753

(a)



Mode 1

Mode 2

Mode 3

Mode 4

Mode 5

754

755

(b)

756

Figure 6: Top view of vibration modes of the four AMT; (a) AMT 1-2 and (b) AMT 3

757

758

759

760

761

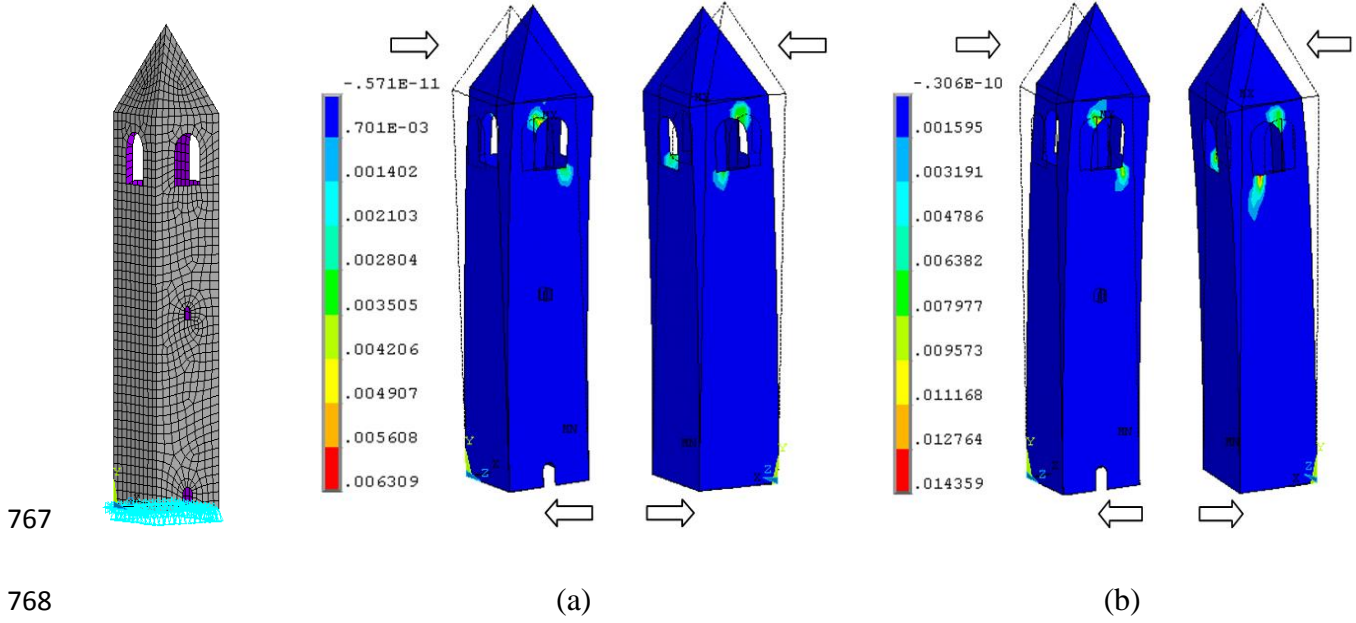
762

763

764

765

766



767
768
769
770
771
772
773
774
775
776
777
778
779
780

Figure 7: Isolated tower masonry roof (AMT 1). Principal plastic strain contours (front and back) at a displacement of: (a) 80 mm (DG 3, SDLS) and (b) 115 mm (DG 4, ULS)

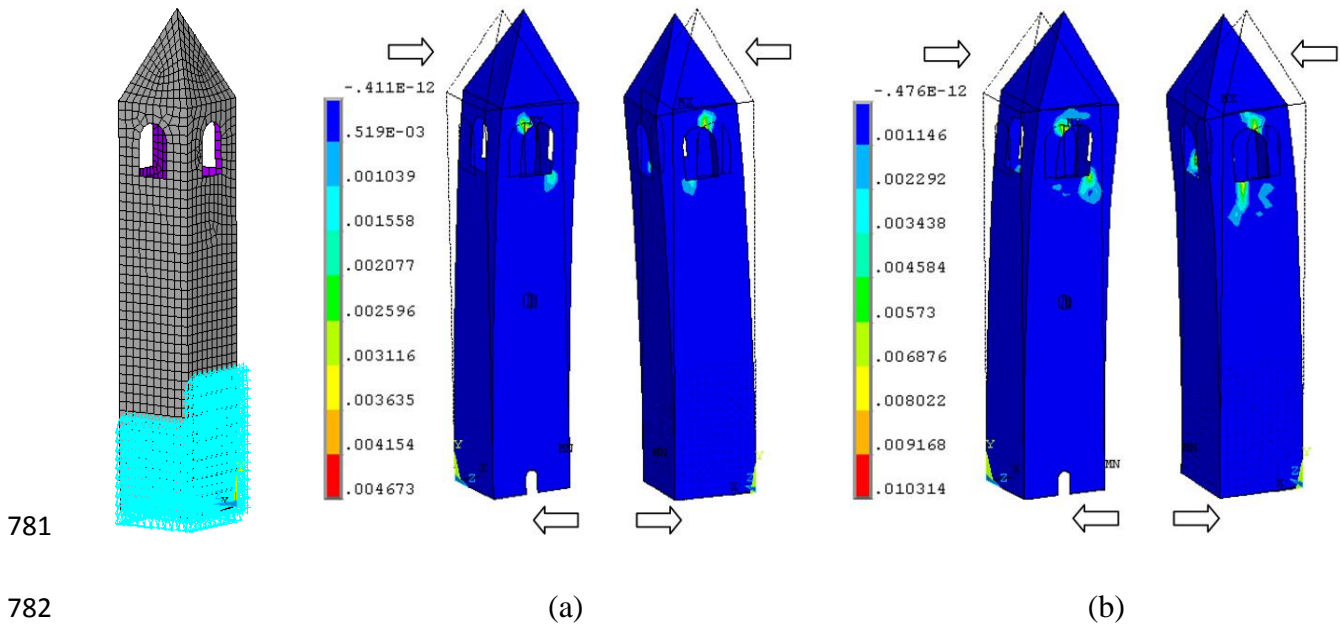
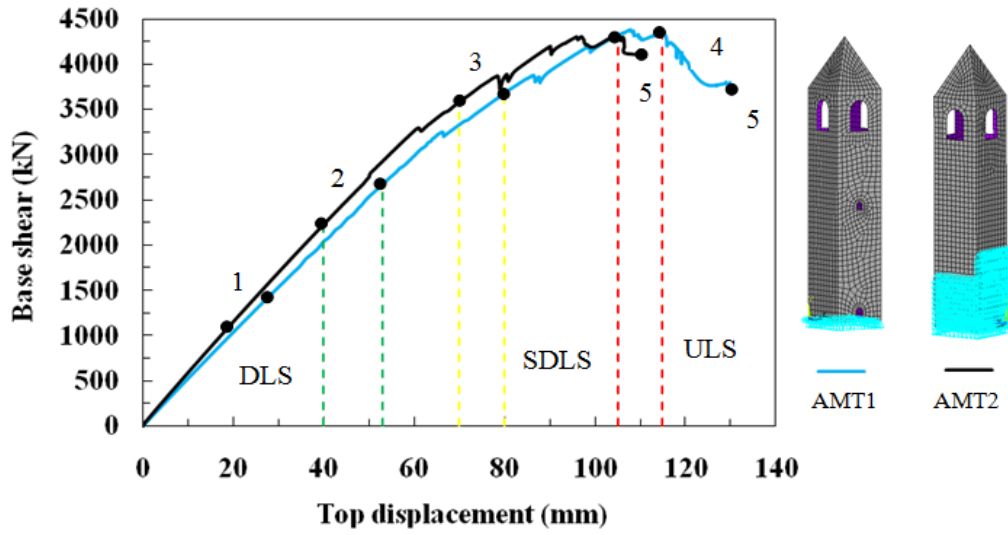


Figure 8: Non-isolated tower masonry roof (AMT 2). Principal plastic strain contours (front and back) at: (a) 70 mm (DG 3, SDLS) and (b) 105 mm (DG 4, ULS)



795

796 Figure 9: Isolated and non-isolated bell towers with masonry roof (AMT 1 and AMT 2). Capacity
 797 curves with the damage grades of the EMS-98 and limit states EC-8

798

799

800

801

802

803

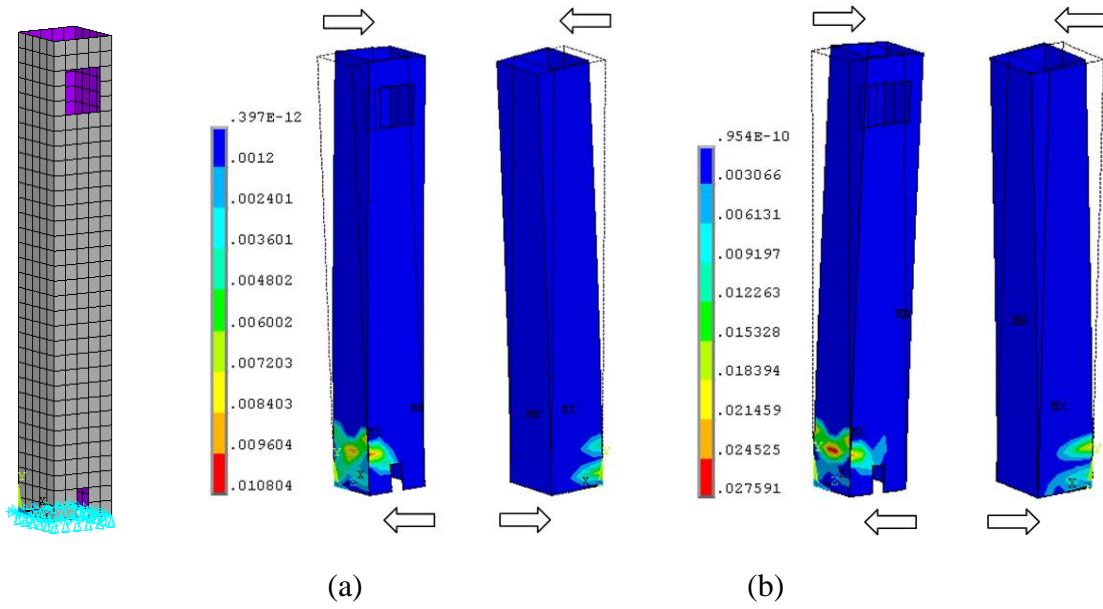
804

805

806

807

808



809

810

811

Figure 10: Isolated bell tower with light roof and openings (AMT 3). Principal plastic strain contours (front and back) at: (a) 185 mm (DG 3, SDLS) and (b) 325 mm (DG 4, ULS)

813

814

815

816

817

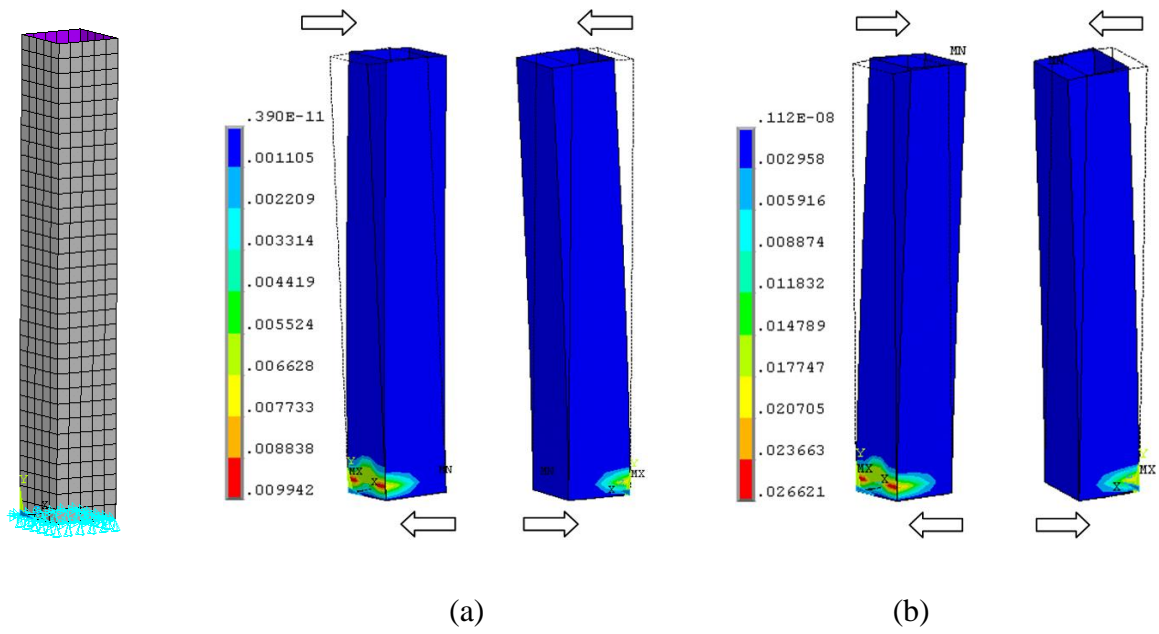
818

819

820

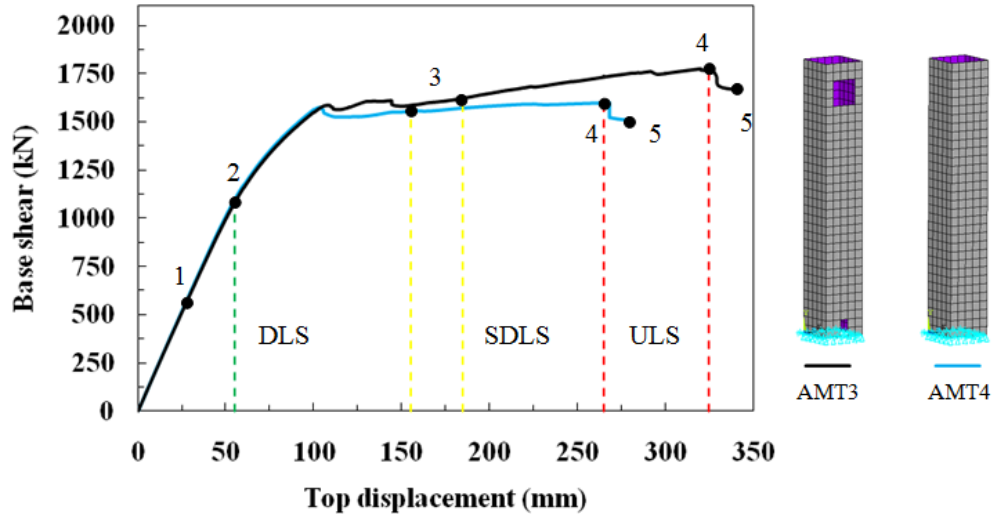
821

822



823
824
825
826
827
828
829
830
831
832
833
834
835
836

Figure 11: Medieval tower light roof (AMT 4). Principal plastic strain contours (front and back) at a displacement of: (a) 155 mm (DG 3, SDLS) and (b) 265 mm (DG 4, ULS)



837

838 Figure 12: Bell and medieval towers with timber roof (AMT 3 and AMT 4). Capacity curves with

839 the five damage grades of the EMS-98 and three limit states of the EC-8

840

841

842

843

844

845

846

847

848

849

850

851 **LIST OF TABLES**

852 Table 1: Summary of dimensions and FEM models of the four AMT

853 Table 2: Natural frequencies of the of the four AMT

854 Table 3: Reference natural frequencies and periods of 10 historical masonry towers

855 Table 4: Summary of masonry inelastic parameters for the material model

856 Table 5: Summary of seismic analyses by the pushover method on the four AMT

857 Table 6: Summary of SCs of the four AMT

858

859

860

861

862

863

864

865

866

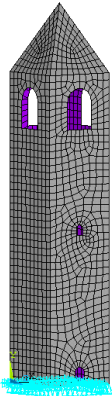
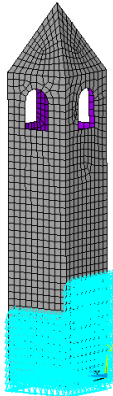

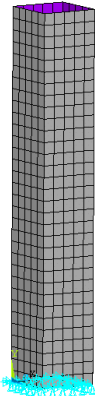
867

868

869

870

Table 1: Summary of dimensions and FEM models of the four AMT

<p>Dimensions in (m)</p> <p>No Scale</p>	 <p>(a)</p>	 <p>(b)</p>	 <p>(c)</p>	 <p>(d)</p>
	AMT 1	AMT 2	AMT 3	AMT 4
Plan	10 x 10	10 x 10	5 x 5	5 x 5
Walls height (thk.)	45 (1.5)	45 (1.5)	32 (1.5)	32 (1.5)
Cover height (thk.)	10 (0.15)	10 (0.15)	-----	-----
Elements (nodes)	2050 (2125)	2050 (2125)	629 (656)	640 (660)
DOF	12627	12627	3876	3900

871

872

873

874

875

876

877

878

879

880

881

Table 2: Natural frequencies of the of the four AMT

Mode no.	Vibration mode	Frequency (Hz)			
		AMT 1	AMT 2	AMT 3	AMT 4
1 st	Bending N-S	1.046	1.293	1.076	1.064
2 nd	Bending E-W	1.051	1.133	1.083	1.064
3 rd	Torsion	3.313	3.702	4.723	4.732
4 th	Bending E-W	3.464	3.464	5.162	5.255
5 th	Bending N-S	3.935	4.138	5.272	5.255

882

883

884

885

886

887

888

889

890

891

892

893

894

895

896

897

Table 3: Reference natural frequencies and periods of 10 historical masonry towers

Reference	Tower height	Frequency (Hz)		Period (sec)	
		1 st	2 nd	1 st	2 nd
Ramos et al. (2010)	20.40	2.15	2.58	0.47	0.39
Bayraktar et al. (2009)	22.00	2.56	2.66	0.39	0.38
Ivorra et al. (2008)	33.90	2.15	2.24	0.47	0.45
Slavik (2002)	35.00	1.10	1.30	0.91	0.77
Ivorra and Pallares (2006)	41.00	1.29	1.49	0.78	0.67
Abruzzese et al. (2009)	41.00	1.26	1.29	0.79	0.78
Lund et al. (1995)	43.50	1.38	1.82	0.72	0.55
Abruzzese et al. (2009)	45.50	1.05	1.37	0.95	0.73
Russo et al. (2010)	58.00	0.61	0.73	1.64	1.37
Gentile and Saisi (2007)	74.10	0.59	0.71	1.69	1.41

899

900

901

902

903

904

905

906

907

908

909

910

911

912

913

Table 4: Summary of masonry inelastic parameters for the material model

Parameter	Value	Unit
σ_m : tensile strength for mortar	0.25	MPa
τ_m : shear strength for mortar	0.35	MPa
c_m : shear inelastic compliance for mortar	1	-
β_m : softening coefficient for mortar	0.7	-
μ : friction coefficient for mortar	0.6	-
σ_M : compressive strength of masonry	2.5	MPa
τ_b : shear strength of units	1.5	MPa
c_M : inelastic compliance of masonry in compression	1	-
β_M : softening coefficient of masonry	0.4	-

914

915

916

917

918

919

920

921

922

923

924

925

926

927

Table 5: Summary of seismic analyses by the pushover method on the four AMT

FEM model reference	Limit states EC-8 and Damage grades EMS-98					
	DLS and DG 2		SDLS and DG 3		ULS and DG 4	
	<i>F</i> (kN)	<i>U</i> (mm)	<i>F</i> (kN)	<i>U</i> (mm)	<i>F</i> (kN)	<i>U</i> (mm)
AMT 1	2700	53	3670	80	4350	115
AMT 2	2220	40	3600	70	4300	105
AMT 3	1100	55	1623	185	1750	325
AMT 4	1100	55	1553	155	1600	265

928

929

930

931

932

933

934

935

936

937

938

939

940

941

942

Table 6: Summary of SCs of the four AMT

FEM model reference	Lateral force (kN)	Vertical loading (kN)	SC
AMT 1	4350	50876	0.086
AMT 2	4300	50876	0.085
AMT 3	1750	18511	0.095
AMT 4	1600	18900	0.085

943